Influence of multiple MISHEMT conduction channels on analog behavior

Bruno G. Canales[1*], Bruno C. S. Sanches[1], Joao A. Martino[1], Eddy Simoen[2], Uthayasankaran Peralagu[3], Bertrand Parvais[3],
Nadine Collaert[3], Paula G. D. Agopian[1,4]
[1] *LSI/PSI/USP, University of Sao Paulo, Sao Paulo, Brazil*
[2] *Ghent University, Belgium*
[3] *imec, Leuven, Belgium*
[4] *UNESP, Sao Paulo State University, Sao Joao da Boa Vista, Brazil*
email*: canales@usp.br

***Abstract* - In this paper, the multiple channels of a MISHEMT device (Metal/Si_3N_4/AlGaN/AlN/GaN - Metal-Insulator-Semiconductor High Electron Mobility Transistor) are studied regarding their impact on basic DC and RF figures of merit. Although most authors treat the 2DEG channel as the MISHEMT main channel, it is shown that its MOS channel contribution to the different RF parameters is of great importance. This unique characteristic makes the MISHEMT RF parameters to be dependent on both V_{GS} and V_{DS}. In relation to a pure 2DEG conduction, the MOS channel is responsible for a large set of analog parameters improvements. It offers an increase of up to 17.6 dB in S21 and of 23 dB in MAG, while sustaining a high f_T and f_{max} for a larger range of V_{GS} and drain current level.**

Keywords - MISHEMT; Multiple Channels; GaN; RF.

I. INTRODUCTION

Wide bandgap semiconductors have been widely used in power electronics [1, 2] due to their ability of operating at high frequencies [3] and at harsh environments [4, 5], showing high power gain at 10 GHz [6]. The GaN Metal-Insulator-Semiconductor High Electron Mobility Transistor (MISHEMT) is one of the promising devices for power applications. In comparison to the HEMT, the MISHEMT also presents high current level, high breakdown voltage and reduced gate current leakage due to the gate insulator [2, 7].

The MISHEMT's heterostructure gives rise to a two-dimensional electron gas (2DEG) [8]. Although the 2DEG at the heterointerface is commonly treated as the main current channel of the MISHEMT, due to the device's gate insulator, depending on its gate biasing, it presents another current channel at the gate insulator/ semiconductor interface as well, whose contribution to the drain current directly influences the device behavior from DC point of view [9]. In this work, we propose the analysis of the basic analog parameters, i.e. intrinsic voltage gain (A_V), Early voltage (V_{EA}) and using the S-parameters, maximum available gain (MAG), unit gain frequency (f_T), maximum oscillation frequency (f_{max}) under the influence of the multiple MISHEMT conduction channels.

II. DEVICE CHARACTERISTICS

Experimental data was obtained by measuring a set of MISHEMTs fabricated in imec – Belgium. The device structures consist of a TiN/Si_3N_4 gate stack over a heterostructure of AlGaN/AlN/GaN grown on a silicon platform. The devices have a width of 40 µm with a W/L ratio of around 100, a 2nm thick insulator, a 15 nm thick barrier, 1 nm thick spacer layer and a 200 µm thick buffer. The RF devices have 2 gate fingers, like two MISHEMTs in parallel. The measured MISHEMTs differ on the distance between its gate and drain electrodes (L_{GD}), shown in Fig. 1, being one short (~750 nm), and one large (~2.5 µm). With a small L_{GD} both channels contribute greatly to drain current (I_D); with a large L_{GD} the MOS channel becomes limited to the gate electrode area, facing a higher series resistance, while the 2DEG extends even more, i.e. the channel length increases. In this case, the main contributor to I_D is the 2DEG. More fabrication details can be found in [1]. The MISHEMT DC electrical characterization was made using the Semiconductor Parameter Analyzer B1500 [10] and its RF characterization was performed using the Keysight PNA Network Analyzer N5227B [11] from 500 MHz to 70 GHz with 100 µm pitch G-S-G microprobes.

III. RESULTS AND ANALYSIS

It is obtained that MISHEMT has a 2DEG channel with an activation voltage ($V_{GS} = V_{t\_2DEG}$) of -4.7 V. The 2DEG channel is distributed between two heterointerfaces, 1 nm distant from each other. At the Si_3N_4/ AlGaN interface it has an accumulation type MOS channel, with an activation voltage ($V_{GS} = V_{t\_MOS}$) of about -1.5 V [12]. Fig. 2 shows the MISHEMT electron concentration under a $V_{GS} > V_{t\_MOS}$ (a), when both 2DEG and MOS channels conduct, $V_{t\_2DEG} < V_{GS} < V_{t\_MOS}$ (b), where the MOS channel faces a high series resistance thus contributing less to I_{DS}, and $V_{GS} < V_{t\_2DEG}$ (c), when the device is shut off. These different conduction mechanisms (2DEG and MOS), shown in Fig. 2, make the MISHEMT capable of offering a higher intrinsic voltage gain (Av) for higher drain voltages (V_{DS}) as shown in Fig. 3, when 2DEG conduction is dominant in the saturation like region. Fig. 4 shows the I_D and transconductance (gm) as a function of gate voltage (V_{GS}). It can be seen that for the device with shorter L_{GD} there is a second increase in I_D for more positive V_{GS}. This is due to the increasing number of electrons in the AlGaN barrier layer and subsequent MOS channel activation, which can be observed in the multiple slope/peaks in gm.

Fig. 5 shows the scattering parameters for the input (S11) and for the output (S22) from 0.5 GHz up to 50 GHz for both devices under V_{DS} = 2 V and different V_{GS}. It is possible to see that for a smaller L_{GD}, S11 tends to be very predictable, while for a larger L_{GD} the input impedance is lower for more positive V_{GS}. The gate and drain capacitances influence more each other on the device with smaller L_{GD}, so its gate impedance has a behavior intertwined with V_{DS} and shows a smoother transition between different V_{GS}. For a large L_{GD} two specific impedance behaviors take place, one before V_{t_2DEG} and one after it, as it is dependent mainly on the 2DEG channel condition. For the larger L_{GD} device, when the 2DEG channel is in its full formation, the channel capacitive behavior attenuates, giving place to a primarily resistive characteristic. This is due to the 2DEG nature, which is made by free electrons detached from their original atoms. Since in this case the MOS channel plays a minor role in I_D, there is no more great change in the output impedance for V_{GS} > -3 V. The device with a short L_{GD} continues to show reasonable changes in S22, as the electrons in the bulk of AlGaN and at the MOS channel are very susceptible to external stress.

A comparison of the devices MAG at 2.4 GHz is shown in Fig. 6, and of transmission coefficient (S21) in Table 1. For more negative gate bias, the curves show that the 2DEG channel length does not affect MAG, which is reasonable because the 2DEG has a specific electron concentration. The MOS channel maintains a high MAG for V_{GS} > -3 V, since it is responsible for a new I_D increase for more positive gate bias. For the V_{GS} of interest of -1 V, where both channels are active in the device with shorter L_{GD} and only the 2DEG channel contributes to I_D of larger L_{GD} device, the increase in S21 for each volt increase in V_{DS} differs substantially for both devices, being bigger for the device with short L_{GD}.

A comparison of the devices f_{max} under different V_{DS} is shown in Fig. 7, and of f_T in Table 2. It can be observed that a shorter 2DEG channel length and the addition of MOS channel on conduction can substantially increase the device RF performance concerning its f_{max} for all gate bias range. The MOS channel can be pointed out as the responsible for extending the device RF performance in relation to f_{max}. Cutoff frequency also substantially increases when the MOS channel is included on conduction. These operation frequencies increase even more from large L_{GD} to short L_{GD} when V_{DS} is higher. The higher free electron movement is responsible for this behavior. When the MOS channel takes place over a great area of the 2DEG channel, it contributes to counter the internal polarizations, so the 2DEG electrons are not constantly being pushed towards the heterointerface.

Fig. 8 shows the f_T and f_{max} curves in relation to I_D for short and large L_{GD} devices. A mobility degradation phenomenon and a consequent gm reduction is observed for all curves with I_D > 20 mA. A short L_{GD} means that the overall channel length is also shorter, as the 2DEG channel is the sum of L_{GD} and MOS channel length. For I_D above 5 mA, the device with short L_{GD} shows a new increase in f_T, given that a shorter channel length presents a higher efficiency. Most of the f_{max} characteristics follow the same f_T behavior in this device, but f_{max} is higher for a larger I_D range. It is important to notice that, as the MOS channel activation offers a new rise in I_D and a new peak in gm, it contributes to a new increase in f_T for more positive V_{GS}.

IV. CONCLUSIONS

This work presents the analog behavior of MISHEMT with a large L_{GD} and short L_{GD} in order to analyze the impact of the multiple MISHEMT conduction channels. The device with short L_{GD} has significant MOS channel contribution while for large L_{GD} it can be considered negligible due to the high series resistance. The S11 shows that a pure 2DEG channel, when fully formed, starts to show a less capacitive behavior and more resistive behavior. The MOS channel, despite being commonly disregarded, plays a leading role on offering higher S21 (3.8 dB against -15.3 dB) and MAG (29 dB against 6 dB) for higher V_{DS}. It also offers high f_T and f_{max} values for a larger span of V_{GS} (from 2 V to 5 V for f_{max}) and I_{DS}. These features are possible due to the MOS channel contribution to new I_{DS} and gm rises.

ACKNOWLEDGMENT

The Brazilian authors acknowledge CNPq, CAPES and grant 2023/14492-4, São Paulo Research Foundation (FAPESP) for the financial support. We also thank Prof. Dr. Gustavo Rehder from LME/PSI/USP for the RF measurements.

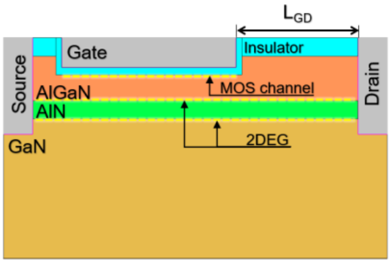

Fig.1 – MISHEMT schematic view.

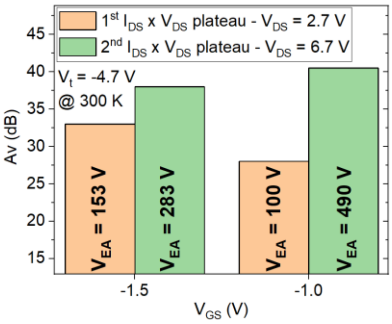

Fig. 3 – Intrinsic voltage gain and Early voltage for different bias conditions.

REFERENCES

[1] U. Peralagu et al., 2019 IEEE IEDM, USA, pp.17.2.1-17.2.4.

[2] M. Van Hove et al., IEEE Electron Device Letters , vol. 33, no. 5, pp. 667-669, May 2012.

[3] S. Yadav et al., 2023 IEDM, San Francisco, USA, 2023, pp. 1-4.

[4] J. He et al., IEEE Electron Device Letters, vol. 43, no. 4, pp. 529-532, April 2022.

[5] W. F. Perina et al, 37th SBMicro, Aug. 2023.

[6] T. Zine-Eddine, et. Al., Journal of Science: Advanced Materials and Devices, vol. 4, Mar. 2019, pp. 180–187.

[7] M. Meneghini et al., Journal of Appl. Phys. vol. 130, June 2021.

[8] K. H. Hamza et al, International Journal of Electronics and Communications, vol. 13, July 2021.

[9] K. Takakura et al. IEEE Trans. On Elect. Dev, vol. 67, Jun. 2020.

[10] Keysight Technologies Semiconductor Device Parameters Analyzer B1500 *Technical Data Sheet 2024*, https://www.keysight. *Com/us/en/assets/7018-01289/data-sheets/5989-2785.pdf*.

[11] Keysight PNA Network Analyzer N5227B *Technical Data Sheet 2024*, https://www.keysight.com/us/en/assets/9018-04327/ *technical-specifications/9018-04327.pdf*

[12] B. G. Canales et al., Semiconductor Science and Technology, vol. 38, n. 11, 2023.

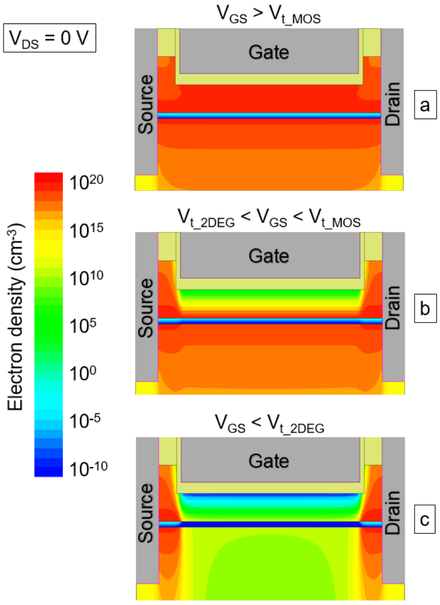

Fig.2 – Multiple channel conditions: 2DEG and MOS channels are enabled (a); 2DEG channel is enabled while MOS channel is disabled (b), and; 2DEG and MOS channels are disabled (c).

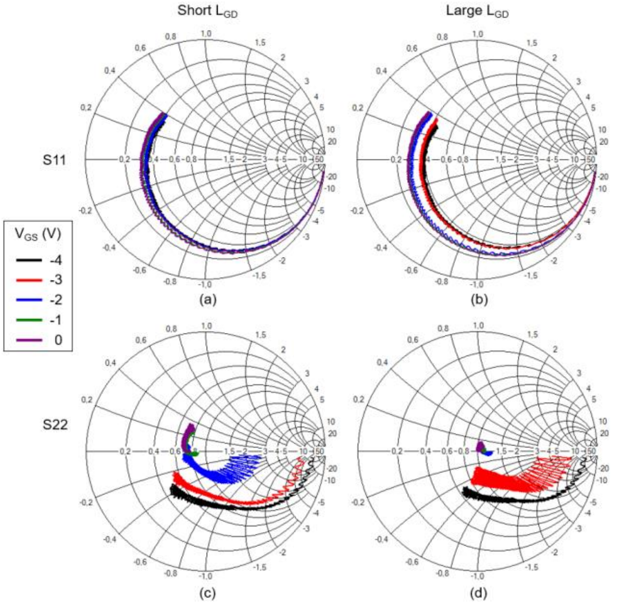

Fig. 5 – S11 for the MISHEMT with short L_{GD} (a) and with large L_{GD} (b). S22 for the MISHEMT with short L_{GD} (c) and with large L_{GD} (d).

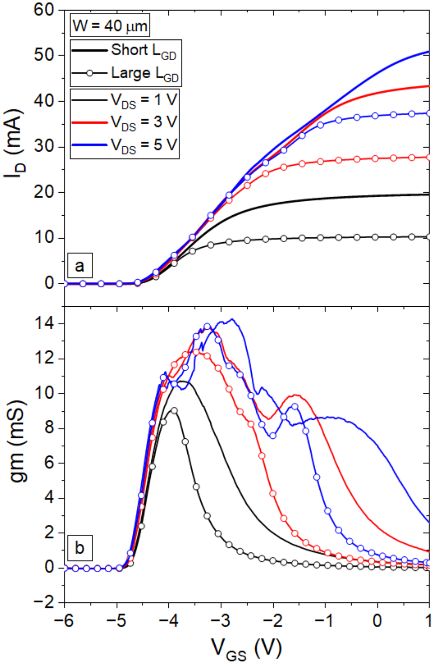

Fig. 4 – Drain current (a) and transconductance (b) as functions of gate voltage for short and large L_{GD} devices and different drain voltages.

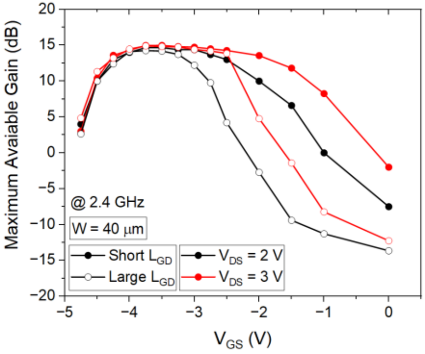

Fig. 6 – MAG as a function of gate voltage of short and large L_{GD} devices operating at 2.4 GHz for different drain voltages.

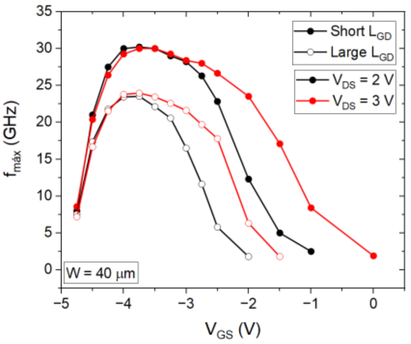

Fig. 7 – f_{max} as a function of V_{GS} of both short and large L_{GD} devices under different V_{DS}.

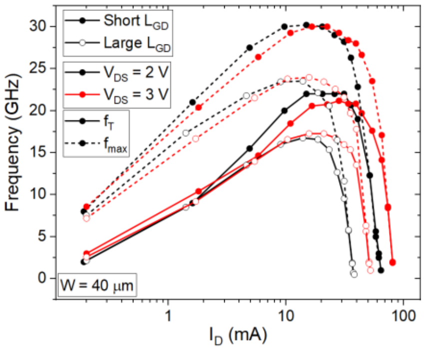

Fig. 8 – f_T and f_{max} as a function of drain voltage for short and large L_{GD} devices and different V_{DS}.

Table 1 – S21 values of short and large L_{GD} devices at V_{GS} = -1 V and different V_{DS}.

V_{GS} = -1 V	S21 for 2.4 GHz (dB)	
V_{DS} (V)	Short L_{GD}	Large L_{GD}
2	-12.0	-23.2
3	-2.0	-19.6
4	3.8	-15.3

Table 2 – f_T values of short and large L_{GD} devices at V_{GS} = -1 V and different V_{DS}.

V_{GS} = -1 V	f_T (GHz)	
V_{DS} (V)	Short L_{GD}	Large L_{GD}
2.0	3.0	0.5
3.0	8.6	1.0
4.0	12.6	2.0